The effect of the recent ^{17}O(p, α)^{14}N and ^{18}O(p, α)^{15}N fusion cross section measurements in the nucleosynthesis of AGB stars[⋆]

S. Palmerini[1,a], M. L. Sergi[1], M. La Cognata[1], L. Lamia[2], R. G. Pizzone[1], and C. Spitaleri[1,2]

[1] *INFN-Laboratori Nazionali del Sud, Catania, Italy*
[2] *Dipartimento di Fisica e Astronomia, Università di Catania, Catania, Italy*

Abstract. The Trojan Horse Method (THM) has been used to investigate the low-energy cross sections of the ^{17}O(p, α)^{14}N and ^{18}O(p, α)^{15}N fusion reactions and to extract the strengths of the resonances that more contribute to the reaction rates at astrophysical energies. Moreover, the strength of the 65 keV resonance in the ^{17}O(p, α)^{14}N reaction, measured by means of the THM, has been used to renormalize the corresponding resonance strength in the ^{17}O + p radiative capture channel. Since, proton-induced fusion reactions on ^{17}O and ^{18}O belong to the CNO cycle network for H-burning in stars, the new estimates of the cross sections have been introduced into calculations of Asymptotic giant branch (AGB) star nucleosynthesis to determine their impact on astrophysical environments. Results of nucleosynthesis calculations have been compared with geochemical analysis of "presolar" grains. These solids form in the cold and dusty envelopes that surround AGB stars and once that have been ejected by stellar winds, come to us as inclusions in meteorites providing invaluable benchmarks and constraints for our knowledge of fusion reactions in astrophysical environments.

1 Introduction

Asymptotic Giant Branch phase (AGB) is the last stage of evolution for low mass stars (M $\leq$ 6M$_\odot$). During this phase H-burning is the main source of energy and it radiatively takes place in a thin shell placed below an extended and cold convective envelope. In this environment products of stellar nucleosynthesis might condensate in grains. Part of these solids, which came to us as inclusions in meteorites felt on the Earth, provide very precise hints of the nucleosynthesis of stars where they formed. Indeed, geochemical analysis can determine the isotopic composition of these solids with an extremely high precision, which is not allowed to stellar spectroscopy.

Oxide grains (Al$_2$O$_3$) of group 1 and 2 have been suggested to condensate, respectively, in the envelopes of RGB[1] and AGB stars, when the C/O ratio is smaller than 1 [1]. The oxygen isotopic mix in these grains provide stringent constraints to the nucleosynthesis of these stars, because of the fragility of ^{18}O and the sensitivity of ^{17}O abundance to temperature. In particular, group 2 grains show ^{18}O/^{16}O ratios lower than expected and ^{17}O/^{16}O ratios larger than accounted for by first dredge-up (FDU, [2, 3]).The convective mixing episode that occurs when a star is approaching the RGB and that is supposed to fix the surface oxygen isotopic abundances in the evolved stages of low mass stars. Furthermore, low ^{12}C/^{13}C and C/N ratios are observed in the spectra of RGB and AGB stars, which are at odds with the predictions of standard stellar evolution models, where only purely convective mixing episodes are considered ([4, 5] and reference therein).

As an explanation for the reported anomalies of C and O isotopic ratios in stellar spectra and presolar grains, [2, 6] suggested a non convective transport mechanism called 'Cool Bottom Process' (CBP) linking the stellar convective envelope to deep layers where H-burning takes place. The common findings of these authors and of the further updates by [7] and [8] are that ^{18}O is destroyed through the ^{18}O(p, α)^{15}N reaction, by mixing phenomena, while the maximum temperature experienced by the circulating material determines the ^{17}O/^{16}O isotopic ratio. In this note we shall concentrate on nucleosynthesis in CBP episodes affecting ^{17}O and ^{18}O abundances in the envelope of low-mass AGB stars (M$\leq$1.5M$_\odot$) using the estimates for the ^{18}O(p,α)^{15}N , ^{17}O(p,α)^{14}N, and ^{17}O(p,γ)^{18}F reaction rate presented by [9–11].

2 Fusion reaction rates determination through the Trojan Horse Method

In RGB and AGB stars the relevant temperatures for the ^{17}O and ^{18}O nucleosynthesis are in the ranges T_9 = 0.01 − 0.1[2]. Thus the cross sections of the 3 fusion reactions of our interest have to be precisely known in the center-of-

---

[1]The Red Giant Branch phase is an evolutionary stage foregoing the AGB, during which the outermost stellar structure already consists in a H-burning shell surrounded by a convective envelope

[2]In this paper we will express the temperature in units of $10^9 K$ adopting the T_9 notation commonly used in Nuclear Astrophysics.

mass energy lower than $E_{c.m.} = 100$ keV. At these energies resonance reactions play a decisive role because the astrophysical S(E)-factor might be dramatically enhanced by the presence of a resonance, whose measurement is then crucial to pin down the astrophysical scenario. However, the presence of the Coulomb barrier, exponentially hampering the cross section at astrophysical energies, and of atomic electrons, shielding the nuclear charges (at least partially), makes the direct measurement of low-energy resonances not accurate enough or even impossible. Indeed the cross section for fusion reactions among charged particles drops below 10^{-12} barn, thus making statistical accuracy and signal-to-noise ratio very poor and the recourse to extrapolation from higher energy mandatory [12, 13]. As a consequence, large uncertainties can be introduced into the astrophysical models because of an incorrect estimate of the relevant cross sections. The THM ([14–16] and references therein) allows one to access the low-energy cross section of an A(x,c)C reaction by extracting the quasi-free (QF) contribution to a suitable A(a,cC)s reaction, having three particles in the exit channel. Particle a, characterized by a prominent $x \oplus s$ cluster structure, is referred to as Trojan horse nucleus as it is used to transfer the participant cluster x. Indeed, if the beam energy is chosen larger than the Coulomb barrier for the A+a interacting system, the breakup of the Trojan horse nucleus takes place inside A nuclear field. The transferred particle x is used to feed the excited states of B, later decaying into c+C. In QF kinematics, the other constituent cluster s is emitted without interacting with the system B, thus behaving as a spectator to the A(x,c)C sub-process. Because the A(a,cC)s reaction is performed at high energies (several tens of MeV), the cross section of the A(x,c)C process is not hindered by the Coulomb interaction of the target-projectile system, while no electron screening enhancement is spoiling the nuclear information [17].

In the energy reagion of our interest the $^{17}O(p, \alpha)^{14}N$ reaction cross section is dominated by two resonances: one at about 65 keV above the ^{18}F proton threshold, and the other at 183 keV. In the last years, the $E_{c.m.} = 183 keV$ resonance has been measured by several authors [18–20]. By contrast, only the direct measurement of the 65 keV resonance performed by [21] was available before of the work by [10], which has determined a resonance strength $\omega\gamma_1 = (3.66^{+0.76}_{-0.64}) \times 10^{-9} eV$ by applying the THM to the quasi-free $^2H(^{17}O, ^{14}N\alpha)n$ reaction and by normalizing experimental data to the weighted average of the three values for the 183 keV resonance strength $\omega\gamma_2 = (1.66 \pm 0.10) \times 10^{-3} eV$, reported in the literature [18, 20, 22]. This result has been used to calculate the contribution of the 65 keV resonance to the total reaction rate adopting the narrow resonance approximation, whose conditions are satisfied for the resonance under investigation [12, 13]. Panel a) of figure 1 shows the ratio (red middle line) between the reaction rate R extracted including the 65 keV resonance strength measured by THM, and the reaction rate R_{Chafa} by [18], also reported in the compilation by [23]. The other red lines mark the position of the upper and lower limits as deduced in [10]. The blue

band represents the Chafa reaction-rate [18] range allowed for by the experimental uncertainties. A small difference ($\sim 20\%$) can be seen in the range $T_9 = 0.02 - 0.1$, while no significant differences are present for $T_9 \geqslant 0.2$, where the contribution of the 65keV resonance to the reaction rate is negligible.

The definition of the resonance strength [12, 13] entails that the $\omega\gamma$ parameter of the $E_1 = 65 keV$ resonance in the $^{17}O(p, \alpha)^{14}N$ reaction is proportional to the proton partial width Γ_p, the exit channel partial width essentially coinciding with the total width, through the statistical factor. Therefore, the 65 keV resonance strength measured by the THM [10] requires a rescaling of the partial width Γ_p and, as a consequence, of the strength of the 65 keV resonance in the $^{17}O(p, \gamma)^{18}F$ channel, being proportional to Γ_p as well:

$$\omega\gamma_p = \frac{2J_R + 1}{(2J_p + 1)(2J_{^{17}O} + 1)} \times \frac{\Gamma_p\Gamma_\gamma}{\Gamma_{tot}} \qquad (1)$$

The TH-scaled resonance strength of the lowest energy resonance is then $\omega\gamma_{p,\gamma}^{THM} = (1.27^{+0.26}_{-0.22}) \times 10^{-11} eV$ to be compared with $(1.64 \pm 0.28) \times 10^{-11} eV$ as given in the recent reviews [18, 23, 24]. Thanks to the THM measurement of the $\omega\gamma_{p,\alpha}$ resonance strength, only the contribution to the reaction rate due to resonance radiative capture can be updated. Furthermore, the resonance THM approach is sensitive to the area subtended by the resonance peak and not to its shape, allowing for the extraction of the strength parameter but not of the S-factor at the Gamow energy, needed to evaluate the tail contribution [12, 13]. However, inside the temperature range $0.006 \geq T_9 \geq 0.06$ (of interest for AGB nucleosynthesis) the contribution of the 65 keV resonance tail to the $^{17}O(p, \gamma)^{18}F$ reaction rate is dominant. The modified $^{17}O(p, \gamma)^{18}F$ reaction rate including the THM-scaled strength of the 65 keV resonance has been obtained by inserting its contribution, in the place of the corresponding one given by [18], into their recommended reaction rate [9]. The THM-modified reaction rate is displayed in Figure 1b as its ratio to the Chafa rate. Figure 1b clearly demonstrates a 20% reduction of the reaction rate at $0.02 \geq T_9 \geq 0.06$.

At temperatures typical of H-burning in AGB stars, the energy interval where the $^{18}O(p, \alpha)^{15}N$ is most effective ranges from about 20 to 70 keV. Though nine resonances show up in the $^{18}O(p, \alpha)^{15}N$ cross section inside the 0–1MeV energy interval, only the 20, 144, and the broad 656 keV resonances are relevant to astrophysics as they determine the reaction rate [25]. Despite several direct experimental investigations [26–28] and many spectroscopic studies [29–32], the reaction rate for this process has considerable uncertainty [25]. Indeed, only the contribution of the 144 keV resonance has been soundly established by [27]. With regard to the 20 keV resonance, its strength was known only from spectroscopic measurements [30] and the direct capture reaction $^{18}O(p, \gamma)^{19}F$ [31]. The values of the resonance strengths in the literature was then affected by large and not-well-defined uncertainties because they are strongly dependent on the optical model potentials adopted in the data analysis. Since the 20 keV
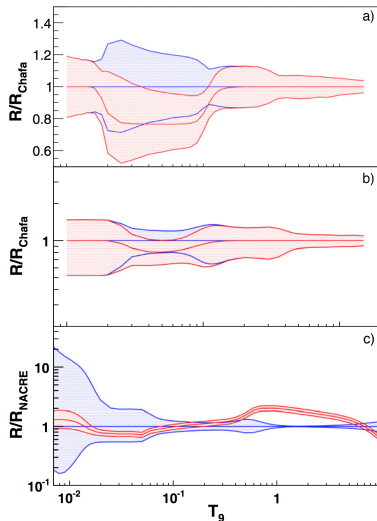
Figure 1. Ratios between the $^{17}O(p,\alpha)^{14}N$, $^{17}O(p,\gamma)^{18}F$ and $^{18}O(p,\alpha)^{15}N$ fusion reaction rates R extracted including resonance strengths measured by the THM, and the reaction rates reported in literature (blue lines [18, 25]). The upper and lower limits account for the uncertainty on the THM-scaled resonance strength. In the same way, a blue band is used to show the uncertainties in the reaction rates by [18, 23] and [25]

resonance is very narrow, according to the measurements in the literature, the narrow-resonance formalism of THM has been employed to obtain its strength [33–35]. By normalizing to the well-known resonance at 144 keV the TH measurement results in $\omega\gamma = (8.3^{+3.8}_{-2,6}) \times 10^{-19}eV$, which is in good agreement with $\omega\gamma = (6^{+17}_{-5}9 \times 10^{-19}eV$, reported by [25] but 10 times more accurate. Indeed, the NACRE-recommended value is based on various kinds of estimates while the THM result is obtained from experimental data, thus the accuracy of the resonance strength has been greatly enhanced. As a cross check, the strength of the 90 keV resonance was extracted as well, leading to $\omega\gamma = (1.76 \pm 0.33) \times 10^{-7}eV$, in good agreement with the strength given by [25], $\omega\gamma = (1.6 \pm 0.5) \times 10^{-7}eV$. Figure 1c shows the ratio of the reaction rate evaluated by means of the THM data to the one in [25]. Clearly, the THM reaction rate shows a much narrower band than the NACRE one over the whole temperature range, especially at low temperatures, thanks to the enhanced precision of the strength of the 20 keV resonance as measured be means of the THM.

3 Effects of the TH reaction rates on RGB and AGB nucleosynthesis

The THM rates of the $^{17}O(p,\alpha)^{14}N$, $^{17}O(p,\gamma)^{18}F$ and $^{18}O(p,\alpha)^{15}N$ fusion reactions have been introduced into the models for proton-capture nucleosynthesis coupled with CBP episodes presented by [8]. To safely analyze the consequences on stellar nucleosynthesis of the new nuclear physics inputs and to avoid uncertainties due to the hypothesis about physical cause of CBP (which are

still subject of debate), the studied rates have been introduced into the parametric model presented by [7–9, 36]. In agreement with these authors, the transport of materials is described by the mixing rate $\dot{M}$ (in units of $10^{-6}M_\odot/yr$) and the temperature T_P of the deepest zones affected by the circulation. We shall refer to this temperature through the logarithmic difference $\Delta T_P = \log T_H - \log T_P$, where T_H is the temperature at which the maximum energy of the H-burning shell is released. In Figure 2, we present a comparison between our results and ones obtained by [8] adopting in calculation the reaction rates described in the previous section and those reported in [23] and [25], respectively. In the figure the black squares along the almost horizontal dashed line report the oxygen isotopic abundances left by the FDU in the envelope of RGB stars with different mass (from 1 to $2M_\odot$ as indicated by the labels). Such values, which have been taken as initial ones for our CBP calculations, do not result to be sensitive to the $^{17}O+p$ or the $^{18}O+p$ reaction rates employed in calculations. Instead, it is clearly shown that, for the same CBP cases, models considering TH data are in better agreement with with the $^{18}O/^{16}O$ versus $^{17}O/^{16}O$ values in group 2 grains. The temporal evolution of chemical abundances under the effect of CBP (during the RGB and AGB phase) are the downward red and black curves, which deal with calculations employing THM measurements and data from [23], respectively. In more detail, the lowest $^{18}O/^{16}O$ values exhibited by group 2 grains can be explained by the most efficient CBP case applied to a $1.2M_\odot$ AGB model (curve b). Under this condition, the resulting isotopic mix in the stellar envelope will closely resemble the one of CNO equilibrium at a temperature T and the $^{17}O/^{16}O$ 'end point' reached by CBP model strongly depends on the mixing depth ΔT_p.

The temporal evolution of ^{17}O abundance during the CNO cycle is determined by the equation

$$\frac{dY(^{17}O)}{dt} = Y(^{16}O)Y(H)R_{^{16}O(p,\gamma)} - Y(^{17}O)Y(H)[R_{^{17}O(p,\alpha)} + R_{^{17}O(p,\gamma)}]$$
(2)

where $Y(i)$ means the abundance in number of the ith isotope and any reaction rate R is temperature and density dependent. From the previous equation, the equilibrium value of the $^{17}O/^{16}O$ ratio turns out to be

$$\frac{Y(^{17}O)}{Y(^{16}O)} = \frac{R_{^{16}O(p,\gamma)}}{R_{^{17}O(p,\alpha)} + R_{^{17}O(p,\gamma)}}$$
(3)

One can notice that equilibrium values of the $^{17}O/^{16}O$ isotopic ratio do not depend on the initial isotopic abundances, but they are instead determined by the values of the reaction rates. As a consequence, in our CBP calculations the $^{17}O/^{16}O$ ratio result larger because of THM cross sections of the $^{17}O +p$ reactions are smaller (see Figure 3, 4 and 5 in [9]) than ones determined reported by [23].

Conversely, no significant changes in the AGB nucleosynthesis predictions arise from the investigation of $^{18}O(p,\alpha)^{15}N$ fusion reaction by means of THM. Indeed CBP calculations adopting $^{18}O(p,\alpha)^{15}N$ reaction rate from [11] and [25] show differences in the final ^{18}O abundances
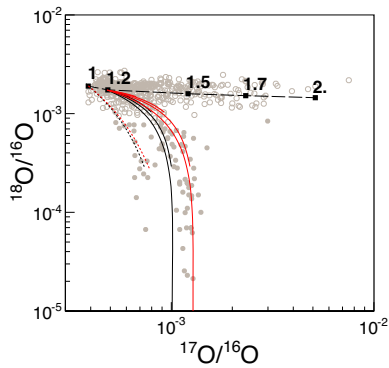
Figure 2. Comparison between the oxygen isotopic mix measured in a sample of oxide grains (from WUSTL Presolar Database: *http://presolar.wustl.edu/?pgd/*) and CBP calculations performed using the model in the paper by [8] for a $1M_\odot$ and a $1.2M_\odot$ solar-metallicity AGB star. The solid curves show the evolution of the O-isotopic ratios in the envelope of the 1.2 $M_\odot$ star calculated for two efficient cases, namely, (a) $\Delta = 0.1$, $\dot{M} = 10^{-6}M_\odot$/yr and (b) $\Delta = 0.1$, $\dot{M} = 3 \times 10^{-6}M_\odot$/yr. The effects of CBP in the composition of the 1 $M_\odot$ (dotted lines) are shown instead just for $\Delta = 0.1$, $\dot{M} = 3 \times 10^{-6}M_\odot$/yr. For both the stellar masses a moderate mixing with $\Delta = 0.22$, $\dot{M} = 10^{-8}M_\odot$/yr. has been considered at play during the previous RGB phase. The CBP calculations executed using the THM $^{18}O(p,\alpha)^{15}N$, $^{17}O(p,\alpha)^{14}N$, and $^{17}O(p,\gamma)^{18}F$ reaction rates are drawn in red, while the results obtained by using the rates by [23].

smaller than the 0.2%. Because of the ^{18}O fragility, which is so easily destroyed that even an increase of about 30% in the rate of the most important destruction channel (namely the $^{18}O(p, \alpha)^{15}N$ reaction) does not produce any appreciable variation. Furthermore, the resulting increase in ^{15}N production is also negligible, in fact in AGB stars ^{15}N is mostly synthesized through the $^{14}N(p, \gamma)^{15}O(\beta^{+})^{15}N$ chain.

4 Results

We have investigated the effect of the recent estimates of the $^{17}O(p,\alpha)^{14}N$, $^{17}O(p,\gamma)^{18}F$ and $^{18}O(p,\alpha)^{15}N$ low-energy reaction rates, on the oxygen isotopic abundances determines by CBP episodes in the envelopes of low mass AGB stars. We confirm the findings by [8] stating that no significant changes occur in the resulting abundances either of ^{15}N or of ^{18}O because of the update of the $^{18}O(p,\alpha)^{15}N$ cross section, while the THM determinations of the $^{17}O+p$ reaction rate increase the $^{17}O/^{16}O$ equilibrium values in the CNO burning by about 30%, with respect to the other measurements reported in literature [23]. This leads to a better agreement between predicted oxygen isotopic ratios and "observational" constraints retrieved from oxide grains. In particular, grains with $^{17}O/^{16}O\leq0.001$ can be better accounted for using the TH data. This finding strengthens the idea that those grains were formed in the envelope of low-mass AGB stars. According to the present work, the upper limit for the progenitor mass should be reduced to 1.2-1.5

$M_\odot$ from 1.5-2 $M_\odot$ as revised by [8], $^{17}O/^{16}O\leq0.0013$ being well reproduced by CBP models applied to an AGB star of 1.2 $M_\odot$ and solar metallicity. Finally, the composition of grains most poor in ^{17}O is accounted for by models assuming that CBP has occurred in a $1M_\odot$ star during the AGB stage and also during previous longer RGB phase. Notice that in the study by [7], where nuclear physics input from [25] were considered, these grains were retined to belong to a 'forbidden' region, which could not be accounted for by nucleosynthesis models.

References

[1] L. R. Nittler *et al.*, Nucl. Phys. A **621**, 113 (1997)

[2] A. I. Boothroyd *et al.*, ApJ **442**, L21 (1995)

[3] B. G. Choi *et al.*, Science **282**, 1284 (1998)

[4] C. Abia *et al.*, A&A **548**, 55 (2012)

[5] R. P. Hedrosa *et al.*, ApJL **768**,11 (2013)

[6] A. I. Boothroyd *et al. ApJ* **430**, L77 (1994)

[7] K. M. Nollett *et al.*, ApJ **582**, 1036 (2004)

[8] S. Palmerini *et al.*, ApJ, **729**, 3 (2011)

[9] S. Palmerini *et al. ApJ*, **764**, 128 (2013)

[10] M. L. Sergi *et al.*, Phys. Rev. C, **82**, 032801 (2010)

[11] M. La Cognata *et al.*, ApJ, **723**, 1512 (2010)

[12] C. Iliadis, Nuclear Physics of Stars (Weinheim: Wiley-VCH Verlag)(2007)

[13] C. Rolfs W. S. and Rodney, Cauldrons in the Cosmos (Chicago, IL: Univ.Chicago Press) (1988)

[14] C. Spitaleri *et al.*, Phys. Rev. C **63**, 055801(2001)

[15] C. Spitaleri *et al.*, Nucl. Phys. A, **834**, 639 (2010)

[16] C. Spitaleri *et al.*, PAN, **74**, 1763 (2011)

[17] M. La Cognata *et al.*, Phys. Rev. C **76**, 065804 (2007)

[18] A. Chafa *et al.*, Phys. Rev. C **75**, 035810 (2007)

[19] C. Fox *et al.*, Phys. Rev. Lett. **93**, 081102 (2004)

[20] B. H. Moazen *et al.*, Phys. Rev. C **75**, 065801 (2007)

[21] J. C. Blackmon *et al.*, Phys. Rev. Lett. **74**, 2642 (1995)

[22] J. R. Newton *et al.*, Phys. Rev. C **75**, 055808 (2007)

[23] E. G. Adelberger *et al.*, Rev. Mod. Phys. **83**, 195 (2011)

[24] C. Iliadis *et al.*, Nucl. Phys. A **841**, 251 (2010)

[25] C. Angulo *et al.*, Nucl. Phys. A **656**, 3 (1999)

[26] H. B. Mak *et al.*, Nucl. Phys. A **304**, 210 (1978)

[27] H. Lorenz-Wirzba *et al.*, Nucl. Phys. A **313**, 346 (1979)

[28] N. S. Christensen *et al.*, NIMPB **51**, 97 (1990)

[29] K. Yagi, J. Phys. Soc. Jpn **17**, 604 (1962)

[30] A. E. Champagne and M. Pitt, Nucl. Phys. A **457**, 367 (1986)

[31] M. Wiescher *et al.*, Nucl. Phys. A **349**, 165 (1980)

[32] C. Schmidt and H. H. Duhm, Nucl. Phys. A **155**, 644 (1970)

[33] M. La Cognata *et al.*, Phys. Rev. Lett. **101**, 152501 (2008)

[34] M. La Cognata *et al.*, PASA **26**, 237 (2009)

[35] M. La Cognata *et al.*, ApJ **708**, 796 (2010)